

Graphical Visualisation of Minimum Energy Requirements for Multi-Effect Distillation Arrangements

Hilde K. Engelen, Sigurd Skogestad

Norwegian University of Science and Technology (NTNU)

Department of Chemical Engineering, 7491 Trondheim, Norway

Abstract

The minimum energy requirements of six different heat-integrated multi-effect and three non-integrated distillation arrangements for separating a ternary mixture have been considered. The focus of the paper is on a heat-integrated complex distillation configuration; called a multi-effect prefractionator arrangement. The comparison of the different arrangements is based on the minimum vapour flowrates at infinite number of stages, which are easily visualised and compared in a V_{\min} -diagram. This tool can be used as a basis for screening and the best arrangement(s) can be studied further using more rigorous simulation methods.

1. Introduction

In the chemical industries, the task of separation is a very energy-consuming process, where distillation is the process most widely used for fluid separations. Distillation columns are used for about 95% of liquid separations and the energy use from this process accounts for an estimated 3% of the world energy consumption (Hewitt et al., 1999). With rising energy awareness and growing environmental concerns there is a need to reduce the energy use in industry. For the distillation process, as it is such a high-energy consumer, any energy savings should have an impact on the overall plant energy consumption.

The use of heat integration combined with complex configurations for distillation columns holds a great promise of energy savings up to about 70%. In addition to saving energy, which are accompanied by reduced environmental impact and site utility costs; there is also a possibility for reduction in capital costs. There are a number of different methods or designs that can be applied to save energy in distillation, for example integration of distillation columns with the background process, heat pumps, multi-effect distillation and complex arrangements such as prefractionators or thermally coupled columns (Petlyuk columns). Deciding which heat integrated arrangement to use is not a straightforward task as the best arrangement is very much dependent on the given separation task and the background process.

In this paper the so-called multi-effect distillation systems are studied. Multi-effect integration is achieved for two or more distillation columns by running one of the columns at a higher pressure and integrating the condenser of this high-pressure (HP) column with the reboiler of the low-pressure (LP) column. The objective of this paper is to present a simple graphical method for obtaining the energy usage and to compare the energy savings with the non-integrated arrangements shown in Figure 1.

For the multi-effect systems there are two modes of integration: forward integration, where the heat integration is in the direction of the mass flow, and backward integration, where the integration is in the opposite direction of the mass flow. The arrangements studied are shown in Figures 2-4. In this paper the focus is on the multi-effect integrated prefractionator arrangement (Figure 4), which has been shown by several authors, for example, Cheng and Luyben (1985) and Emtir et al. (2001) to have high energy savings, compared with other distillation arrangements.

An easy form of comparison for the energy consumption is the minimum vapour flowrate, which are often given as simple shortcut equations. Such equations are given for different integrated multi-effect arrangements by Rév et al. (2001). Relationships for the prefractionator can be found in e.g. Carlberg and Westerberg (1989).

A visual representation of the minimum vapour flowrate of the fully thermally coupled (Petlyuk) arrangement has been presented by Halvorsen (2003a), Fidkowski (1986) and Christiansen (1997). In these diagrams the vapour flowrate is plotted against the distillate/feed ratio in the prefractionator column. Defining the feed composition and the relative volatility of the components being separated, the diagram can be drawn by simply plotting five points (see Figure 5). The diagram can be used to find the minimum vapour flowrate for the Petlyuk column, as well as the recovery for the preferred split.

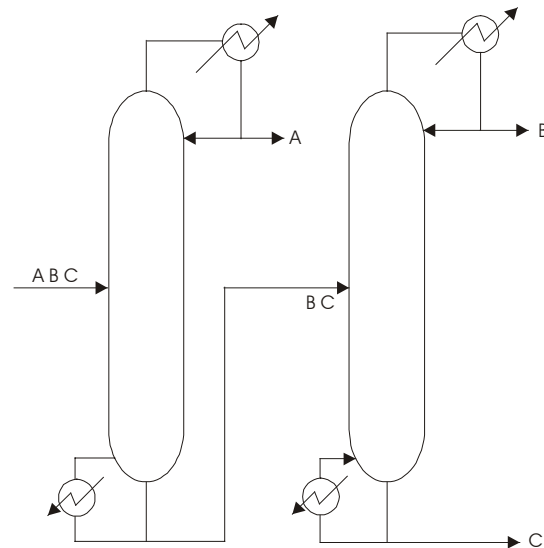
As shown in this paper, the V_{\min} -diagram developed for the Petlyuk columns can be used for multi-effect heat-integrated systems if it is modified to also include the minimum vapour flowrate for a sharp binary A/B and B/C split. The diagram can then be used to find the minimum vapour flowrate for all six multi-effect columns in Figure 2-Figure 4. Also it can be used to obtain and to find further information about the multi-effect heat integrated prefractionator arrangement, such as the optimal recovery of middle component, if the columns are balanced and compare the savings from the integrated arrangement with the Petlyuk arrangement.

2. Multi-Effect Arrangements

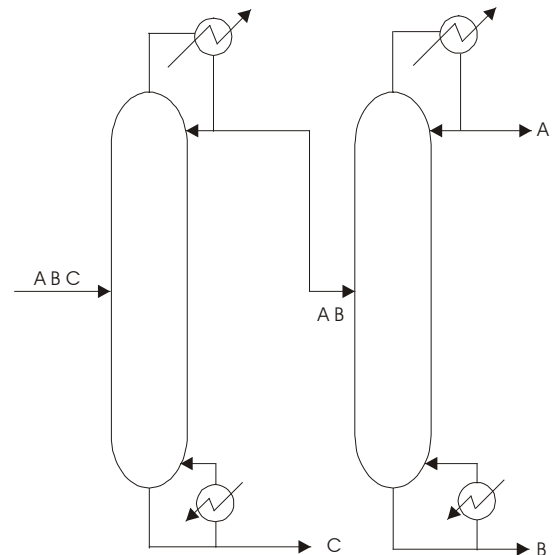
Figure 1 shows four non-heat-integrated schemes for separation of a ternary mixture (ABC): a direct split (DS) arrangement, an indirect split (IS) arrangement, a prefractionator (P) arrangement and a directly coupled prefractionator (Petlyuk) arrangement. In the DS arrangement (Figure 1a) the lightest component (A) is split off in the first column. For the IS arrangement (Figure 1b) the heaviest component (C) is split off in the first column. For the prefractionator and Petlyuk arrangement (Figure 1c and Figure 1d) the split in the first column is between the lightest (A) and the heaviest (C) component, with the middle component (B) distributing between the two products.

Figure 1. Non-heat integrated schemes for separating a ternary mixture (ABC)

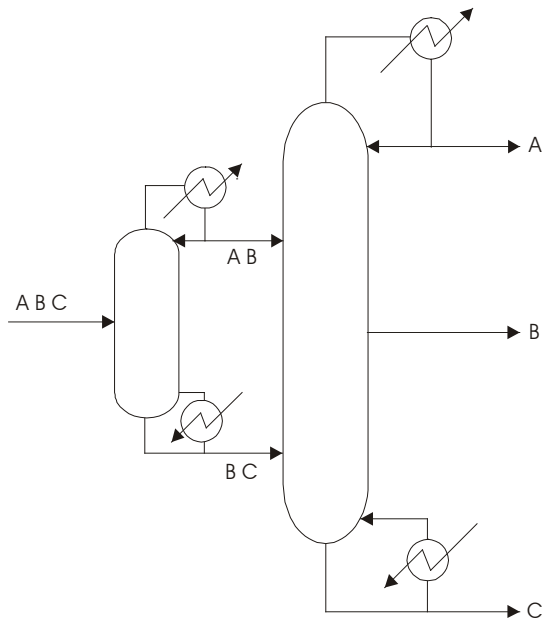
a) Direct split (DS) arrangement



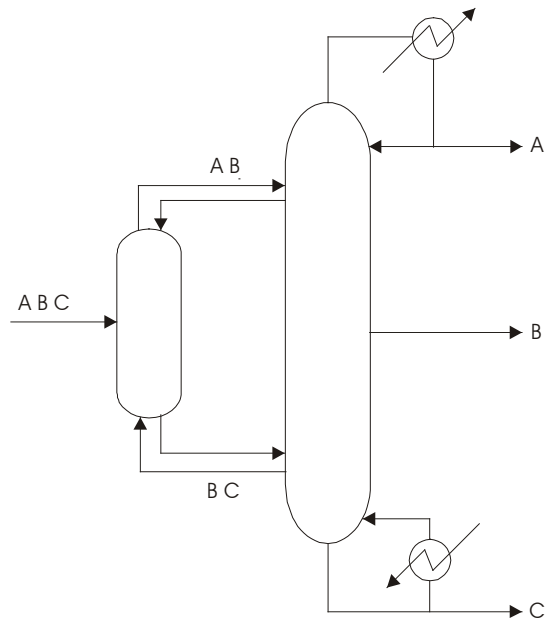
b) Indirect split (IS) arrangement



c) Prefractionator arrangement



d) Petlyuk arrangement



The three first arrangements shown in Figure 1 can be heat integrated in a multi-effect fashion by running one column at a higher pressure and then combining the condenser of the high-pressure (HP) column with the reboiler of the low-pressure (LP) column. Each of these can be integrated in a forward or backward fashion, giving us 6 different schemes to consider:

- 1) **Direct split columns.** Two possible configurations are possible for the direct split: a forward integration (DSF) as in Figure 2a and a backward integration (DSB) as in Figure 2b.
- 2) **Indirect split columns.** Two possible configurations are possible for the indirect split: a forward integration (ISF) as in Figure 3a and a backward integration (ISB) as in Figure 3b.
- 3) **Prefractionator arrangement.** The two column options considered are; a forward split (PF), see Figure 4a and a backward split (PB), see Figure 4b.

Figure 2. Multi-effect direct split arrangements

- a) Direct split with forward integration (DSF) b) Direct split with backward integration (DSB)

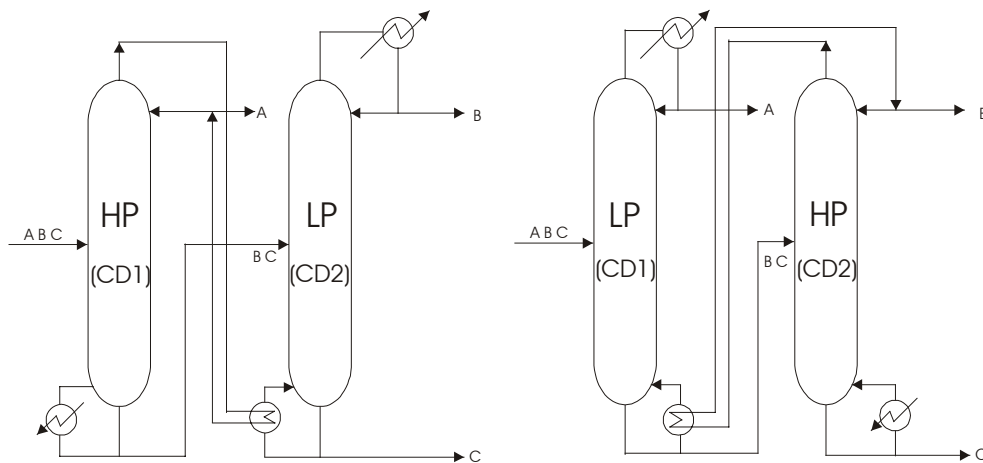


Figure 3. Multi-effect indirect split arrangements

- a) Indirect split with forward integration (ISF) b) Indirect split with backward integration (ISB)

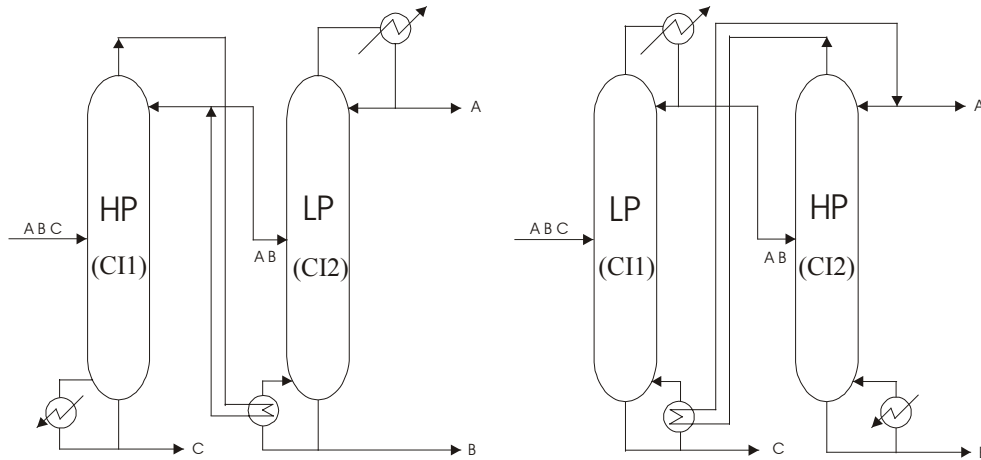
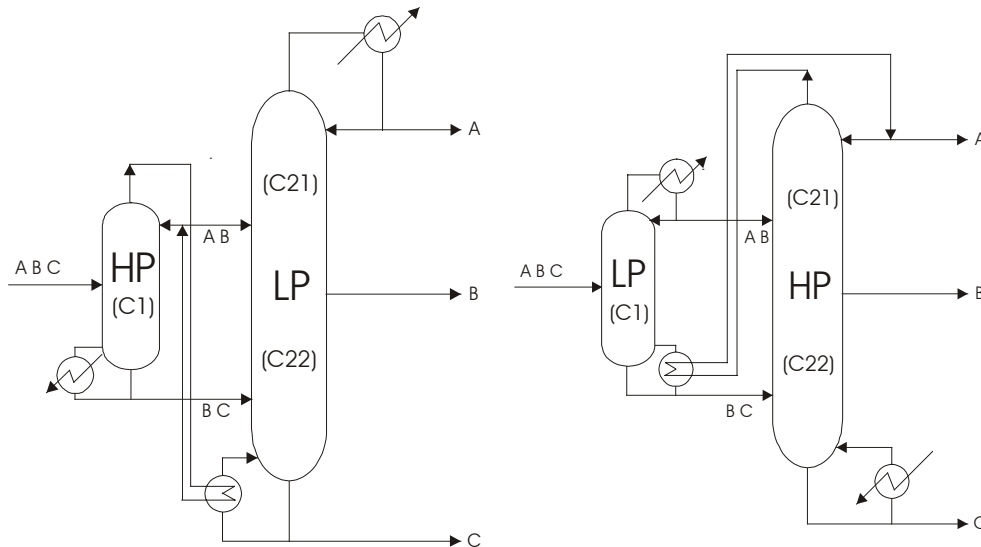


Figure 4. Multi-effect prefractionator arrangements

- a) Prefractionator with forward integration (PF) b) Prefractionator with backward integration (PB)



It should be noted that an additional scheme is available for the prefractionator design if the separation is carried out in three columns with three pressure levels. This arrangement, called a *dual* scheme, has not been considered here, as the energy consumption is the same as for the two-column multi-effect prefractionator arrangement and as this three-column arrangement would result in a higher capital cost.

In all cases the products and flows between the integrated columns are assumed to be liquid. This may seem non-optimal, but because of the multi-effect integration there is no advantage in using vapour flows between these columns. This follows because (i) it is better to supply the vapour in the reboiler (ISF, PF) and (ii) it is not economical to compress vapour going from the LP to the HP column (ISB, PB).

3. Minimum Vapour Flow (Energy Requirement)

In the following we consider ideal mixtures where we can assume constant relative volatility (α_i constant) for the vapour liquid equilibrium and constant molar flows for the energy balance. For all short-cut equations sharp splits are assumed and the vapour flowrate (V) is the bottom flowrate, unless otherwise stated.

The minimum energy required is obtained using column sections with an infinite number of stages. This provides a useful target for distillation where one easily can get within 10% of this target with a reasonable number of stages.

The feed data required for the shortcut calculations are the flowrate (F) and the composition (z), which in this paper has been defined as $[z_A z_B z_C]$ for the ternary mixture ABC. In addition we require the relative volatilities between the components $[\alpha_{AC} \alpha_{BC} \alpha_{CC}]$, which are referenced to the heaviest component (C), so $\alpha_{CC} = 1$. Also needed is the feed liquid fraction, q , where $q = 1$ is liquid feed and $q = 0$ is vapour feed.

3.1. Minimum Vapour Flow Expressions (Underwood & King)

For a multi-component mixture the vapour flowrate for a given separation can be calculated using Underwood's equations (e.g. King, 1980). The *minimum vapour flowrate* (V_{\min}) at the top of the column is given as:

$$V_{T,\min} = \sum_{i=1}^{N_c} \frac{\alpha_{iH} x_{i,D} D}{\alpha_{iH} - \theta} \quad (1)$$

where $x_{i,D}$ is the distillate composition of component i , α_{iH} is the relative volatility with respect to the heaviest component H and θ is the Underwood root. For a mixture of N_c components the $(N_c - 1)$ Underwood roots θ are found as the solution of the so-called feed equation:

$$(1 - q) = \sum \frac{\alpha_{iH} z_i}{\alpha_{iH} - \theta} \quad (2)$$

Here z_i is the feed composition of component i and q is the liquid fraction of the feed. The roots lie between the values of neighbouring relative volatilities so: $\alpha_{1H} > \theta_1 > \alpha_{2H} > \theta_2 > \alpha_{3H} > \theta_3 > \dots > \alpha_{N_c-1H} > \theta_{N_c}$. Equation (2) applies for minimum reflux conditions when there are infinite number of stages in the column.

In the *ternary separations* ($N_c = 3$) considered here we first compute the $(N_c - 1) = 2$ roots from the feed equation (Equation 2). This gives θ_A and θ_B , which are the same for all the configurations. The root to be used in Equation (1) depends on the split between the components and thus on the configurations considered. If we have a sharp A/BC split as for the DS configurations, then we use θ_A and if we have a sharp AB/C split as for the IS configurations, then we use θ_B in Equation (1).

For the special case of a binary separation with components i and j the minimum vapour flowrate at the top of the column ($V_{T,\min}$) for infinite number of stages can be calculated by using Kings formula (King, 1980):

$$V_{T,\min} = \frac{r_{i,D} - \alpha_{ij} r_{j,D}}{\alpha_{ij} - 1} F + D \quad (3)$$

Here $r_{i,D}$ and $r_{j,D}$ are the recoveries of components i and j in the distillate, where the recovery of component i is defined as $r_{i,D} = x_{i,D} D / z_i F$. For a liquid feed the vapour flowrate at the top of the column equals the vapour flowrate at the bottom ($V_{B,\min}$) and for a sharp split we have $r_{i,D} = 1$ and $r_{j,D} = 0$. The minimum vapour flowrate for a binary sharp split with liquid feed is then:

$$V_{T,\min} = \frac{1}{\alpha_{ij} - 1} F + D \quad (4)$$

Note that for liquid feed the vapour flow in the top, V_T equals the vapour flow in the bottom, V_B . Otherwise, if $q \neq 1$ the vapour flowrate in the top is given as: $V_T = V_B + (1-q)F$.

For the ternary separation of ABC the relative volatilities of interest are α_{AC} and α_{BC} . For the binary AB and BC separations the relative volatilities of interest are $\alpha_{AB} = \alpha_{AC}/\alpha_{BC}$ and α_{BC} . If the relative volatilities then varies with pressure different relative volatilities should be used in the HP and LP column. In the V_{\min} equations we use the notation α_{AB}' or α_{BC}' to indicate that the relative volatilities are actually at different pressure levels.

3.2. Minimum Vapour Flowrate for Multi-Effect Arrangements

The minimum vapour flow required for the multi-effect configurations in Figure 2-Figure 4 can be found using the shortcut equations described above. It should be noted that when assuming constant relative volatility independent of pressure the multi-effect configurations with the same split type have the same minimum vapour flow requirements, i.e. DSF = DSB, ISF = ISB and PF = PB. However, if the relative volatility is assumed to be a function of the pressures (and therefore temperatures) in the columns then the relative volatility in the HP and LP columns are different. The V_{\min} equations remain the same, but using different volatilities for the HP and LP columns will give different minimum vapour flowrate for same split configurations, i.e. DSF \neq DSB, ISF \neq ISB and PF \neq PB.

With the assumptions of liquid flows, we have from Equations (1) and (4) that the minimum vapour flowrate for the individual columns in the direct-split arrangements (DSF and DSB) in Figure 2 are:

$$V_{\min}^{CD1} = \frac{\alpha_{AC} z_A}{\alpha_{AC} - \theta_A} F \quad (5)$$

$$V_{\min}^{CD2} = \frac{F}{\alpha'_{BC} - 1} (z_B + z_C) + \frac{z_B}{z_B + z_C} \quad (6)$$

The required minimum vapour flowrate for the multi-effect **integrated direct split configurations** is equal to the highest vapour flowrate requirement in the individual columns, i.e.:

$$V_{\min,DSF} = V_{\min,DSB} = \max \{ V_{\min}^{CD1}, V_{\min}^{CD2} \} \quad (7)$$

To compare, for the **non-integrated direct split configuration** (Figure 1a) the minimum vapour flowrate is the sum of the required vapour rates in each column:

$$V_{\min,DS} = V_{\min}^{CD1} + V_{\min}^{CD2} \quad (8)$$

For the indirect-split arrangements ISF and ISB (Figure 3) the vapour flowrate for the individual columns is expressed as:

$$V_{\min}^{CI1} = \left(\frac{\alpha_{AC} z_A}{\alpha_{AC} - \theta_B} + \frac{\alpha_{BC} z_B}{\alpha_{BC} - \theta_B} \right) F \quad (9)$$

$$V_{\min(q=1)}^{CI2} = \frac{F}{\alpha'_{AB} - 1} (z_A + z_B) + z_A F \quad (10)$$

For the multi-effect **integrated indirect split configurations** with **forward and backward integration** the minimum vapour flowrate required is then the maximum of the two flowrates in the individual columns:

$$V_{\min,ISF} = V_{\min,ISB} = \max \{ V_{\min}^{CI1}, V_{\min(q=1)}^{CI2} \} \quad (11)$$

To compare with the non-integrated arrangement (Figure 1b) we note that here it is better to partially condense the vapour from the first column so the feed to the second column is vapour ($q = 0$). We have:

$$V_{\min(q=0)}^{C12} = \frac{F}{\alpha'_{AB} - 1} (z_A + z_B) \quad (12)$$

So the minimum vapour flowrate for the **non-integrated indirect split configuration** (Figure 1b) is then:

$$V_{\min,IS} = V_{\min}^{C11} + V_{\min(q=0)}^{C12} \quad (13)$$

We next consider the prefractionator arrangement (Figure 4). In the prefractionator column (C1) there is a sharp split between the lightest (A) and the heaviest (C) component (A/C), i.e. $x_{A,D}D = z_A F$ and $x_{C,D} = 0$ in Equation (1). However, from Equation (1) the minimum vapour flowrate will depend on the amount of the middle (B) component in the distillate, as expressed by $x_{B,D}$. This can alternatively be expressed in terms of the product split from the prefractionator column:

$$\eta \triangleq \frac{D^{C1}}{F} \quad (14)$$

Note that $x_{B,D}D = F(\eta - z_A)$ so from Equation (1) V_{\min} will depend linearly on η .

Furthermore, Equation (2) gives two possible Underwood roots (θ_A and θ_B) and the two corresponding values of V_{\min} are from Equation (1):

$$V_{\min(\theta=\theta_A)}^{C1} = \left(\frac{\alpha_{AC} z_A}{\alpha_{AC} - \theta_A} + \frac{\alpha_{BC} (\eta - z_A)}{\alpha_{BC} - \theta_A} \right) F \quad (15)$$

$$V_{\min(\theta=\theta_B)}^{C1} = \left(\frac{\alpha_{AC} z_A}{\alpha_{AC} - \theta_B} + \frac{\alpha_{BC} (\eta - z_A)}{\alpha_{BC} - \theta_B} \right) F \quad (16)$$

Note the linear dependency on η . In the prefractionator the minimum vapour flowrate as a function of the recovery, η , is the maximum of these two (Fidkowski, 1986):

$$V_{\min}^{C1}(\eta) = \max \left(V_{\min(\theta=\theta_A)}^{C1}, V_{\min(\theta=\theta_B)}^{C1} \right) \quad (17)$$

This gives a V-shaped curve as a function of η and the minimum vapour flowrate in the prefractionator column occurs at a specific value of $\eta_{\text{preferred}}$, called "the preferred split".

However, to find the optimal value of η for the multi-effect arrangement we also have to consider the vapour flow required in the main column. The two sections of the main column performs sharp binary separations and from Equation (4) the minimum vapour flowrate in the upper section (C21) of the main column is:

$$V_{\min}^{C21}(\eta) = \left[\frac{\eta}{\alpha'_{AB} - 1} + z_A \right] F \quad (18)$$

and in the lower section (C22):

$$V_{\min}^{C22}(\eta) = \left[\frac{1-\eta}{\alpha'_{BC} - 1} + (1-\eta - z_C) \right] F \quad (19)$$

Note again the linear dependency on η .

As column sections C21 and C22 are connected the minimum vapour flowrate in the main column is the maximum of the two. The minimum flowrate of the integrated prefractionator arrangement (Figure 4) is the maximum of the main column and the prefractionator and by adjusting η we have:

$$V_{\min,PF} = V_{\min,PB} = \min_{\eta} \left[\max \left\{ V_{\min}^{C1}(\eta), V_{\min}^{C21}(\eta), V_{\min}^{C22}(\eta) \right\} \right] \quad (20)$$

The "optimum" recovery η occurs at the lowest minimum vapour flowrate for the system.

To compare, for the non-integrated prefractionator arrangement (Figure 1c) we have:

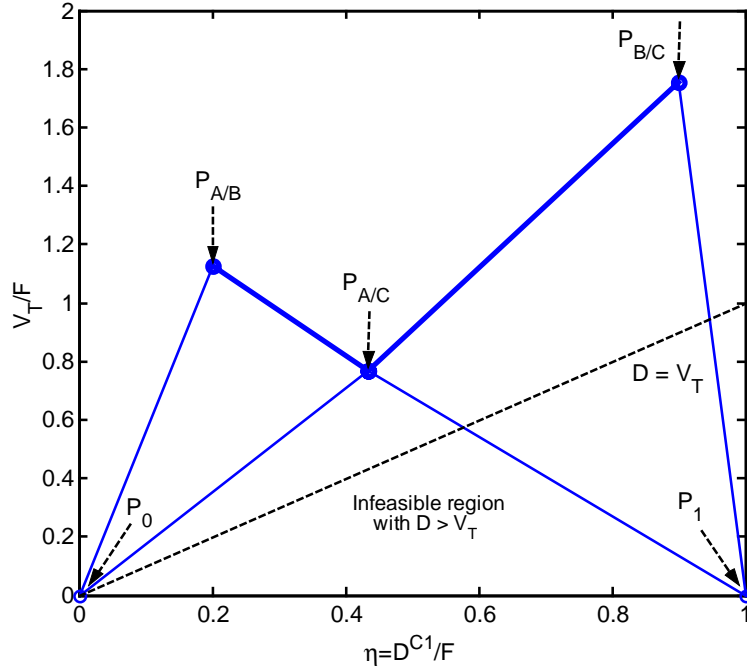
$$V_{\min,P} = \min_{\eta} \left[V_{\min}^{C1}(\eta) + \max \left\{ V_{\min}^{C21}(\eta), V_{\min}^{C22}(\eta) \right\} \right] \quad (21)$$

However, here it turns out the minimum vapour flow requirement is always at the "preferred split" ($\eta = \eta_{\text{preferred}}$). For the integrated prefractionator arrangements the preferred split will only be optimal in some cases (see below).

4. Visualising the Vapour Flow Requirements in a V_{\min} -Diagram

From the above equations we see that a plot of V_{\min} against the prefractionator split $\eta = D^{C1}/F$ will result in straight lines. This observation is the basis for the proposed V_{\min} -diagram previously used by Halvorsen and Skogestad (2003a) for the Petlyuk column. In this section, we show how to draw the diagrams for the multi-effect arrangements and their use is then discussed in Sections 5 and 6.

Figure 5. V_{\min} diagram for ternary separation.



To draw the V_{\min} -diagram in Figure 5 for the prefractionator column (C1) we have to identify five points $[\eta, V_{T,\min}/F]$. For sharp splits and liquid feeds these are from the equations above (see also Halvorsen and Skogestad, 2003a):

$$P_{AB} : \left[z_A, \frac{\alpha_{AC} z_A}{\alpha_{AC} - \theta_A} \right] \quad (22)$$

$$P_{BC} : \left[z_A + z_B, \frac{\alpha_{AC} z_A}{\alpha_{AC} - \theta_B} + \frac{\alpha_{BC} z_B}{\alpha_{BC} - \theta_B} \right] \quad (23)$$

$$P_{AC} : \quad \left[\eta_{preferred}, \frac{\alpha_{AC} z_A}{\alpha_{AC} - \theta_B} + \frac{\alpha_{BC} (\eta_{preferred} - z_A)}{\alpha_{BC} - \theta_B} \right] \quad (24)$$

Point P_{AC} is at the "preferred" split where:

$$\eta_{preferred} = z_A - \frac{\alpha_{AC} z_A (\alpha_{BC} - \theta_A) (\alpha_{BC} - \theta_B)}{\alpha_{BC} (\alpha_{AC} - \theta_A) (\alpha_{AC} - \theta_B)} \quad (25)$$

Finally, we have points P_0 and P_1 . These are actually not used in this paper, but they complete the diagram for the prefractionator:

$$P_0 : \quad = [0, 0] \quad (26)$$

$$P_1 : \quad = [1, (1 - q)] \quad (27)$$

In the V_{min} -diagram (Figure 5) the peak $P_{A/B}$ is the minimum vapour flow for a sharp split between A/B with C present (A/BC) and the peak $P_{B/C}$ gives the minimum vapour flow for a sharp B/C split with A present (AB/C). The curve between the points P_{AB} - P_{AC} - P_{BC} gives the minimum vapour flowrate for sharp split between A and C for different recoveries of B in the distillate from the prefractionator. Along and above this line the split between A and C is sharp, with B distributing between the top and bottom product. The "preferred split" at point $P_{A/C}$ gives the minimum vapour flowrate for a sharp split between the lightest component (A) and the heaviest component (C) in the prefractionator. Note that below the dotted line where $D = V_T$ the separation in the prefractionator is infeasible as we must have that $V_T < D$.

For the Petlyuk column the minimum vapour flowrate is the highest of the peaks in the V_{min} diagram (Halvorsen and Skogestad, 2003a), i.e.:

$$V_{min, Petlyuk} = \max[V_{A/B}, V_{B/C}] \quad (28)$$

where $V_{A/B}$ and $V_{B/C}$ correspond to the points $P_{A/B}$ and $P_{B/C}$, respectively, in Figure 5.

The diagram in Figure 5 corresponds to the prefractionator column (C1) in Figure 4. In Figure 6 the V_{min} -diagram is extended to the entire multi-effect arrangement by including the relationships for the minimum vapour flowrate in the two sections of the main column.

The additional four co-ordinates for the extended diagram are for the main column sections C21 and C22. They are found from the minimum vapour flowrate expression (Equation 4) for binary separation with sharp splits and liquid feed:

The two points $[\eta, V_{T, min}/F]$ for the **upper section of the main column, (C21)**, are:

$$P_{M1} : \quad \left[z_A, \frac{z_A}{\alpha'_{AB} - 1} + z_A \right] \quad (29)$$

$$P_{M2} : \quad \left[z_A + z_B, \frac{z_A + z_B}{\alpha'_{AB} - 1} + z_A \right] \quad (30)$$

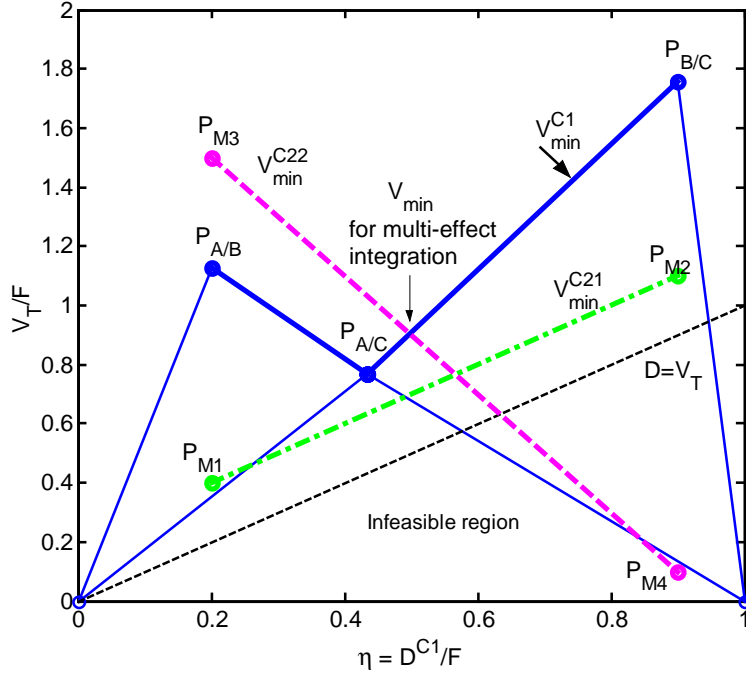
and the two points for the **lower section of the main column, (C22)**, are:

$$P_{M3} : \quad \left[z_A, \frac{z_B + z_C}{\alpha'_{BC} - 1} + z_B \right] \quad (31)$$

$$P_{M4} : \quad \left[z_A + z_B, \frac{z_C}{\alpha'_{BC} - 1} \right] \quad (32)$$

It should be noted that in Figure 6 the lines for V^{C21} and V^{C22} go from $\eta = z_A$ (points P_{M1} and P_{M3}) to $\eta = z_A + z_B$ (points P_{M2} and P_{M4}). To the left of points P_{M1} and P_{M3} there is no B present in the feed to the upper part of the main column so all of B goes to the lower part of the main column. To the right of points P_{M2} and P_{M4} all of B is fed to the upper part of the main column and no B goes to the lower part.

Figure 6. Extended V_{\min} diagram for the multi-effect prefractionator arrangement in Figure 4 (Case 1).



5. Using the V_{\min} -Diagram for the Multi-Effect Prefractionator Column

In the multi-effect prefractionator arrangement in Figure 4 the vapour flow in all the three column sections must be equal. It then follows that the minimum vapour flow for a *given* recovery of component B in the prefractionator (given value of $\eta = D^{C1}/F$) is the maximum of the minimum flowrates in the three sections. The value of η should be adjusted such that V_{\min} is minimised. The minimum vapour flow for the multi-effect prefractionator arrangement is then:

$$V_{\min,PF} = V_{\min,PB} = \min_{\eta} \left[\max \left\{ V_{\min}^{C1}(\eta), V_{\min}^{C21}(\eta), V_{\min}^{C22}(\eta) \right\} \right] \quad (33)$$

Importantly, this value can easily be found using the V_{\min} -diagram in Figure 6, as is further illustrated in Table 1.

When we require sharp split the points $P_{A/B}$, $P_{A/C}$ and $P_{B/C}$ span the minimum vapour flowrate for the prefractionator column (shown in bold). The points for the main column are shown as P_{M1} - P_{M2} (C21) and P_{M3} - P_{M4} (C22). For the specific case in Figure 6 the minimum vapour flow as a function of η , $V_{\min,PF}(\eta)$, follows the V_{\min}^{C22} -line from the point P_{M3} and down to the crossing with the V_{\min}^{C1} -line and then goes up to the point $P_{B/C}$. The minimum vapour flowrate for the overall multi-effect integrated prefractionator arrangement is then where the V_{\min}^{C22} and V_{\min}^{C1} -lines cross (indicated as V_{\min} in the figure).

The case shown in Figure 6 is referred to as Case 1. More generally, we have the following five possibilities for the multi-effect prefractionator arrangements:

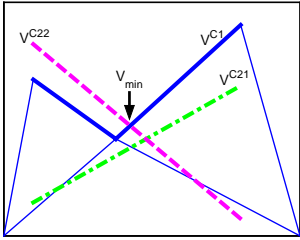
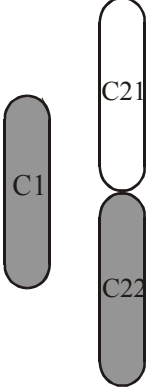
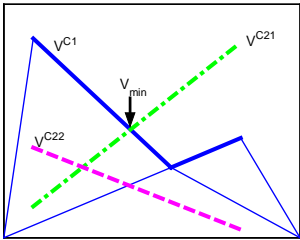
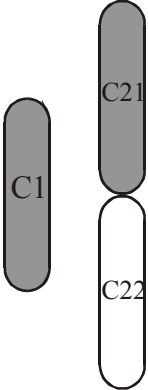
- Case 1: Lines for V^{C22} and V^{C1} cross at optimum: $V^{C1} = V^{C22} > V^{C21}$
- Case 2: Lines for V^{C21} and V^{C1} cross at optimum: $V^{C1} = V^{C21} > V^{C22}$

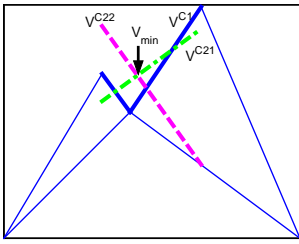
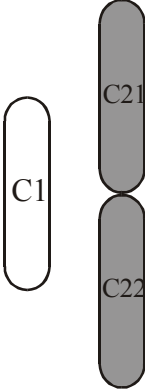
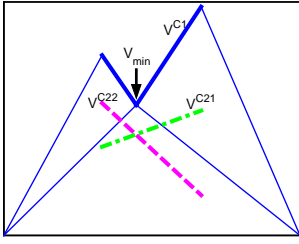
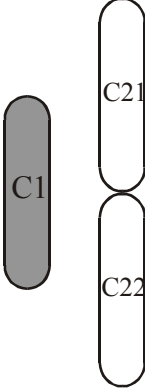
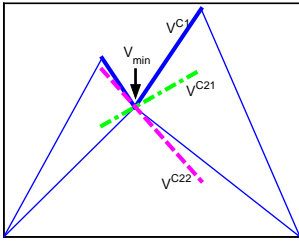
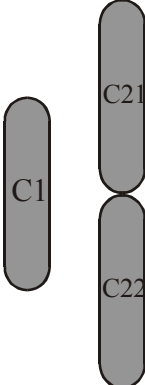
- Case 3: Lines for V^{C21} and V^{C22} cross at optimum: $V^{C21} = V^{C22} > V^{C1}$
- Case 4: Optimum at "preferred split", no lines cross: $V^{C1} > V^{C21}$ and V^{C22}
- Case 5: All lines cross in the same point at optimum: $V^{C1} = V^{C21} = V^{C22}$

The left column in Table 1 shows the V_{\min} -diagrams for these different cases. We can also use the information from the V_{\min} -diagram to find the column sections that receive excess vapour ("unbalanced sections"). The column sections receiving excess vapour are shown in white in the middle column in Table 1. The "limiting" column sections, which operate at minimum flows, are shown in grey.

Except for Case 5 there will always be an excess (or "unbalance") of vapour flow requirement in some column section. The last column of Table 1 summarises the design or operational options that are available for the different classes. Note that the options available can differ depending on the arrangement, PF or PB, used. The difference occurs as for the PF arrangement the heat input is to the prefractionator column (C1) whereas for the PB arrangement the heat input is to the lower section of the main column (C22).

Table 1 Possible V_{\min} -diagrams for multi-effect prefractionator arrangement (note: white sections receive excess vapour, i.e. are over-refluxed).

V_{\min} -diagram	Limiting column sections	Possible use of excess vapour
<p>Case 1 ($V^{C1} = V^{C22} > V^{C21}$)</p> 		<p><u>PF</u></p> <ul style="list-style-type: none"> a) Intermediate condenser between C22 and C21. b) Overpurify C21 product. c) Vapour sidestream product. d) Shorter column section C21. <p><u>PB</u></p> <ul style="list-style-type: none"> a) Overpurify C21 product. b) Shorter column section C21.
<p>Case 2 ($V^{C1} = V^{C21} > V^{C22}$)</p> 		<p><u>PF</u></p> <ul style="list-style-type: none"> a) Overpurify C22 product. b) Shorter column section C22. <p><u>PB</u></p> <ul style="list-style-type: none"> a) Intermediate reboiler between C22 and C21. b) Overpurify C22 product. c) Shorter column section C22.

<p>Case 3 ($V^{C21} = V^{C22} > V^{C1}$)</p> 		<p><u>PF</u> Not common, unless α increases with pressures.</p> <p><u>PB</u> Overpurification in C1 is possible, but not important for final products.</p> <p>a) Use shorter column C1 b) Intermediate condenser at top of C21.</p>
<p>Case 4 ($V^{C21} = V^{C22} < V^{C1}$)</p> 		<p><u>PF</u> a) Intermediate condenser between C22 and C21, or between C1 and C22. b) Overpurify products from main column. c) Vapour sidestream product. d) Shorter column sections C21 and C22.</p> <p><u>PB</u> Not common, unless α increases with pressures.</p>
<p>Case 5 ($V^{C1} = V^{C1} = V^{C22}$)</p> 		<p>All column sections are balanced. No special measures needed.</p>

6. V_{\min} -Diagram for Other Column Configurations

The V_{\min} -diagram can also be used to find the **minimum vapour flowrate** of other column arrangements. This is shown in Figure 7 for the following multi-effect arrangements:

- Direct split with forward and backward integration (DSF/DSB).
- Indirect split with forward and backward integration (ISF/ISB).

The minimum vapour flowrate for the DSF/DSB arrangement in Figure 7 is the maximum of the two points $P_{A/B}$ and P_{M3} . For the ISF/ISB arrangement the minimum vapour flowrate is the maximum of the two points $P_{B/C}$ and P_{M2} . The difference between these points will also indicate how the columns are unbalanced. It is easy to see from the diagram which of the integrated DS or IS arrangement has the lowest energy demand.

We have here assumed no difference in the relative volatilities for the forward and backward integrated cases, so that $V_{DSF} = V_{DSB}$ and $V_{ISF} = V_{ISB}$. If the relative volatilities are expected to vary with pressure

then different relative volatilities for the HP and the LP column should be used (this will give different V_{\min} -diagrams for the different same split arrangements).

The V_{\min} -diagram can also be used to find the minimum vapour flowrate for the non-integrated single pressure direct split (DS) and indirect split (IS) arrangements. The minimum vapour flowrate for direct split is the sum of ($P_{A/B} + P_{M3}$) and for the indirect split (IS) the sum of ($P_{B/C} + P_{M2}$). Finally, minimum vapour flowrate for the Petlyuk column is, as mentioned earlier, the maximum of the peaks ($P_{A/B}, P_{B/C}$).

In summary we then have, with reference to Figure 7:

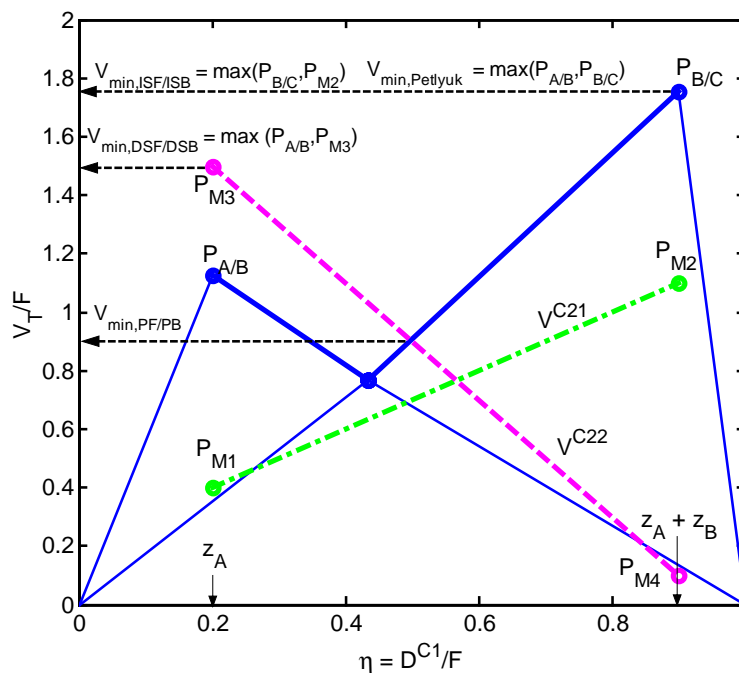
DS(non-integrated):	$V_{\min} = P_{A/B} + P_{M3}$	
IS(non-integrated):	$V_{\min} = P_{B/C} + P_{M2}$	
DSF/DSB:	$V_{\min} = \max[P_{A/B}, P_{M3}]$	
ISF/ISB:	$V_{\min} = \max[P_{B/C}, P_{M2}]$	
Petlyuk (non-integrated):	$V_{\min} = \max[P_{A/B}, P_{B/C}]$	
PF/PB:	$V_{\min} = \min_{\eta} \left[\max \left\{ V_{\min}^{C1}, V_{\min}^{C21}, V_{\min}^{C22} \right\} \right]$	(see Table 1)

The above summary, together with Figure 7 provides the main contribution of this paper.

The V_{\min} -diagram in Figure 7 can thus be used as a screening method to quickly determine if multi-effect distillation (especially that with a prefractionator) should be investigated further.

From the shape of the V_{\min} -diagram it can be seen that with the constant relative volatility assumption (independent of pressure) the multi-effect prefractionator arrangement (PF/PB) will always be better than the other multi-effect arrangements considered here. It will also always be better than the non-integrated arrangements, including the Petlyuk column. This is further confirmed by the data in Table 2.

Figure 7. Use of V_{\min} -diagram to find minimum vapour flowrate for various column arrangements, with relative volatility independent of pressure.



7. Case Studies

7.1. Minimum Vapour Flowrate Using Shortcut Equations

Table 2 summarises some results for different distillation arrangements when calculating the minimum vapour flowrate using the shortcut equations described in Section 3, assuming constant relative volatility independent of pressure, liquid feed, constant molar flows and sharp splits.

The minimum energy requirement (V_{\min}) is expressed as the percentage improvement compared to the best of the non-integrated direct (DS) or indirect split (IS) arrangements. The conventional non-heat integrated and multi-effect arrangements are considered, as well as the Petlyuk arrangement. The results are presented for five different feeds (equimolar feed, feeds with large amount of the intermediate component, feed with a small amount of the intermediate component and a feed with large amount of the lightest component) and five different relative volatilities. The relative volatilities considered for the different feed cases are; equal difficulty between A/B and B/C, difficult A/B, difficult B/C, difficult A/B and B/C and easy A/B and B/C.

From these results the following general observations were made, in terms of "*first law*" energy requirements:

- The integrated prefractionator arrangements are always better than the other arrangements.
- The highest energy savings for the integrated prefractionator arrangements occur when there is a high concentration of the middle component in the feed. The percentage savings for some of the cases exceed 70 %. The highest savings, when there is a high concentration of B, is when the relative volatilities are more or less "balanced" (i.e. same level of difficulty between the A/B and B/C separation).
- The lowest energy savings for all arrangements are when the feed contains a lot of the light component (A), or small amounts of heavy component (C), or small amounts of the middle component.
- There is generally a large difference between the integrated prefractionator arrangements and the Petlyuk arrangement, which is the best non-integrated arrangement (Halvorsen, 2003c). The improvement of the Petlyuk column ranges from about 5 % to 47 %, depending on the difficulty of separation and feed composition. The lowest savings are when there is a large amount of light component in the feed and the highest savings are when there is a high amount of the middle component in the feed.

For the calculations in Table 2 the same relative volatility has been used for both columns. This is the simplest assumption and it is in agreement with the assumption of equal heat of vaporisation made when assuming constant molar flows. For real mixtures, the relative volatility is usually reduced when we increase the pressure, but this is not always the case (e.g. mixture of methanol and ethyl acetate).

Table 2. Energy savings in percent compared with the best of the conventional DS or IS (without multi-effect heat integration), assuming α constant with pressure

z_F	Column Arrangement	$\alpha = [4 \ 2 \ 1]$	$\alpha = [5 \ 4.5 \ 1]$	$\alpha = [5 \ 1.5 \ 1]$	$\alpha = [2 \ 1.5 \ 1]$	$\alpha = [10 \ 5 \ 1]$
1/3	DS	-1.94	0.00	-4.98	0.00	-0.28
	IS	0.00	-0.51	0.00	0.00	0.00
	Petlyuk	32.80	7.59	12.76	39.54	32.71
	DSF/DSB	47.26	7.59	25.56	39.54	32.71
	ISF/ISB	32.80	8.21	12.76	44.65	34.03
	PF/PB	61.73	37.44	47.41	59.06	50.05
0.10	DS	-0.09	0.00	-0.23	0.00	-0.01
	IS	0.00	-0.03	0.00	0.00	0.00
	0.80 Petlyuk	32.99	11.39	12.43	47.37	44.23
	0.10 DSF/DSB	37.69	11.39	16.20	47.34	49.62
	ISF/ISB	32.99	11.63	12.43	49.02	44.23
	PF/PB	65.55	52.83	54.54	71.71	71.80
0.20	DS	0.00	0.00	-1.06	0.00	0.00
	IS	-0.66	-0.49	0.00	-2.11	-0.52
	0.60 Petlyuk	33.40	8.50	13.41	40.03	37.72
	0.20 DSF/DSB	48.91	8.50	25.70	40.03	37.72
	ISF/ISB	33.40	8.89	13.41	43.12	38.53
	PF/PB	64.43	42.87	52.40	62.01	57.39
0.45	DS	-6.25	0.00	-17.42	0.00	-0.78
	IS	0.00	-1.38	0.00	0.00	0.00
	0.10 Petlyuk	34.38	4.53	14.19	34.78	18.39
	0.45 DSF/DSB	34.38	4.53	27.74	34.78	18.39
	ISF/ISB	34.38	4.90	14.19	39.13	19.26
	PF/PB	42.58	18.40	37.29	45.65	26.45
0.80	DS	0.00	0.00	0.00	0.00	0.00
	IS	-10.25	-2.14	-3.75	-17.43	-4.07
	0.10 Petlyuk	14.96	1.73	19.04	12.45	8.10
	0.10 DSF/DSB	14.96	1.73	29.55	12.45	8.10
	ISF/ISB	15.23	1.77	19.04	12.86	8.18
	PF/PB	19.92	10.78	32.34	19.68	13.27

7.2. Analysis of a given Mixture Using V_{\min} -diagrams

The V_{\min} -diagram is here used to analyse a mixture of benzene, toluene and m-xylene. The relative volatilities for this mixture are given in Table 3. In this example we have included pressure variations in the relative volatility, which is important for practical considerations. The relative volatilities used have been calculated at HP = 6 bar and LP = 1 bar, using a commercial simulation package. The pressure of 6 bar in the HP column has been selected as it gives a sufficient temperature driving force between the multi-effect integrated columns. For the main column the relative volatilities given are for the upper section of the main column, α'_{AB} and for the lower section of the main column, α'_{BC} .

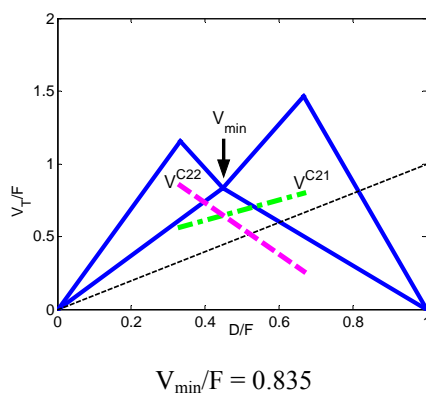
Table 3. Relative volatilities for mixtures

	Forward integration (PF)			Backward integration (PB)		
	Prefractionator (LP) C1	Main column (HP)		Prefractionator (HP) C1 (HP)	Main column (LP)	
		C21	C22		C21	C22
Benzene	3.58	2.43		5.57	1.90	1.88
Toluene	1.88	1.00	2.29	2.29	1.00	1.00
m-xylene	1.00		1.00	1.00		

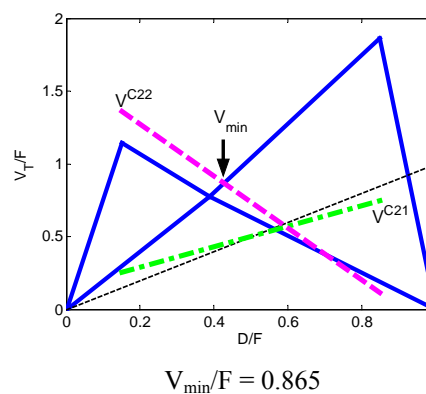
Figure 8 shows the V_{\min} -diagrams for this mixture using the forward-integrated prefractionator arrangement (PF) at two different feed compositions: $z_F = [1/3 \ 1/3 \ 1/3]$ and $z_F = [0.15 \ 0.7 \ 0.15]$. Figure 9 shows the same mixture and feed compositions, but for the backward-integrated arrangement (PB). Note that the reason for the difference between the PF and PB arrangement is the dependency of the relative volatility on the pressure. For the PF system the high-pressure column is the prefractionator, whereas for the PB system the high-pressure column is the main column. The relative volatilities used reflect this difference.

Figure 8. V_{\min} diagram for selected mixture using a PF arrangement (α depends on pressure).

a) $z_F = [1/3 \ 1/3 \ 1/3]$ - Case 4-PF



$z_F = [0.15 \ 0.7 \ 0.15]$ - Case 1-PF



It can be seen from Figure 8a, that at equimolar feed the minimum energy demand in the prefractionator column is higher than the minimum energy demand in both sections of the main column. The main column will then have to run at a higher reflux than necessary, with the result that

the column can be made shorter (due to the trade off between reflux and number of stages). Alternatively the products in the main column can be overpurified.

In the case of the feed with the high concentration of the middle component the energy demand in the prefractionator and the lower section of the main column is balanced (see Figure 8b). The energy demand in the upper section of the main column is less than the other two sections. In this case there are two options: to use a fewer number of stages in the upper section (and higher reflux) or to use an intermediate condenser between the upper and lower section of the main column. A third option would be to overpurify the light component.

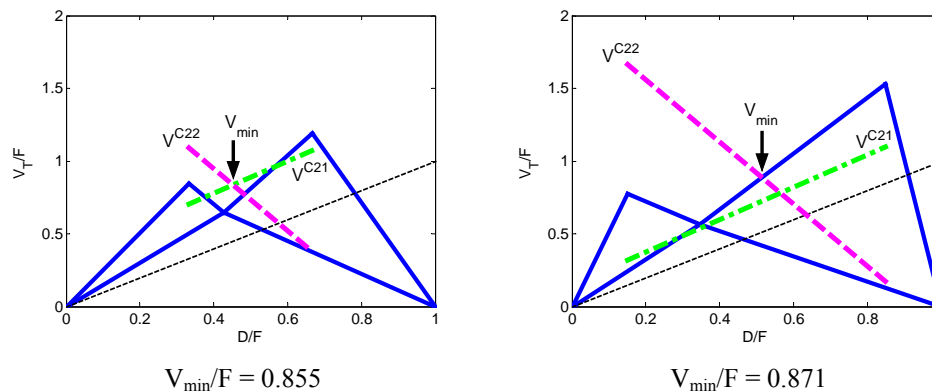
For the equimolar feed using the PB arrangement the minimum energy demand in the main column is higher than in the prefractionator (see Figure 9a). This is a backward integrated scheme so the main column is used to boil the prefractionator column. There are two options for balancing the columns: to condense some of the vapour at the top of the main column or to run the prefractionator column at a higher reflux and use fewer stages.

For the feed with the high concentration of the middle component the upper section of the main column has a lower vapour flow demand. We can not install an intermediate condenser between the two column sections and the prefractionator requires a higher vapour flow than the upper section. The option will be to reduce the number of stages in the upper section while running at the higher reflux rate. Another option would be to overpurify the light product.

Figure 9. V_{min} diagram for Mixture 1 using PB arrangement (α depends on pressure).

a) $z_F = [1/3 \ 1/3 \ 1/3]$ - Case 3-PB

$z_F = [0.15 \ 0.7 \ 0.15]$ - Case 1-PB



7.3. Conclusions

Shortcut equations for minimum vapour flow in ternary multi-effect distillation systems have been presented. Using these shortcut equations it was shown that the multi-effect prefractionator arrangement is always better than the other multi-effect arrangements considered, when assuming constant relative volatility, constant molar flows, liquid feeds and sharp splits.

The energy saving of the multi-effect prefractionator was also shown in a V_{min} -diagram. For a prefractionator or Petlyuk column a V_{min} -diagram can be plotted to show the minimum vapour flowrate as a function of the distillate flowrate, when there are infinite number of stages in the columns. For a ternary mixture it has been shown how this diagram can be extended to include heat-integrated multi-effect arrangements. It has been shown how the V_{min} -diagram then can be used to find the minimum vapour flowrate for all conventional non-integrated and multi-effect integrated arrangements. Figure 7 summarises these results in a single V_{min} -diagram.

From both the shortcut equations and the V_{min} -diagram it was shown that the multi-effect prefractionator has the lowest energy consumption compared with the other arrangements studied.

The calculation of V_{min} assumes infinite number of stages, however, this is not in itself an important limitation since the actual value of V is usually close to V_{min} . Thus, V_{min} provides a good target for comparing energy usage for alternative arrangements. Of course, when the selecting the best

arrangements one must also consider other factors such as capital cost, operability and control, product flexibility, available utilities and other often case-to-case specific requirements.

The formulas for the points in the V_{\min} -diagrams have in this paper been given for sharp splits but they can easily be extended to non-sharp splits (see Halvorsen and Skogestad, 2003b). The lines in the V_{\min} -diagram will remain straight, but they will be shifted slightly down, but usually not much since V_{\min} is proportional to the purity, e.g. V_{\min} for 98% purity is 98 % of that for sharp separation splits. The main effect of purity is on the required number of stages, which increases in proportion to the log of the impurity (e.g. Skogestad, 1997).

The main assumption in this paper is that of constant relative volatility and constant molar flows. For real mixtures, similar diagrams may be generated by simulation.

7.4. References

- Biegler, L.T., Grossman, I.E., Westerberg, A.W., 'Systematic Methods of Chemical Process Design', Prentice Hall PTR, 1997.
- Carlberg, N.A., Westerberg, A.W., 'Temperature-heat diagrams for complex columns. 3. Underwood's method for the Petlyuk configuration', *Ind. Eng. Chem. Res.*, 1989, 28, 1386-1397.
- Cheng, H. C., Luyben, W., 'Heat-integrated distillation columns for ternary separations', *Ind. Eng. Chem. Process Des. Dev.*, 1985, 24, 707-713.
- Christiansen, A.C., 1997, 'Studies on optimal design and operation of integrated distillation arrangements', PhD. Thesis, Norwegian University of Science and Technology.
- Emtir, M., Rév, E., Fonyó, Z., 'Rigorous simulation of energy integrated and thermally coupled distillation schemes for ternary mixture', *Applied Thermal Engineering*, 2001, 21, 1299-1317.
- Fidkowski, Z., Krolikowski, L., 'Thermally coupled system of distillation columns: optimization procedure', *AIChE Journal*, 1986, Vol. 32, No. 4, 537-546.
- Halvorsen, I.J., 'Minimum Energy Requirements in Complex Distillation Arrangements', PhD. Thesis Norwegian University of Science of Technology (NTNU), 2001.
- Halvorsen, I.J., Skogestad, S., 'Minimum energy consumption in multicomponent distillation. 1. V_{\min} diagram for a two product column', *Ind. Eng. Chem. Res.*, 2003a, 42, 596-604.
- Halvorsen, I.J., Skogestad, S., 'Minimum energy consumption in multicomponent distillation. 2. Three product Petlyuk arrangements', *Ind. Eng. Chem. Res.*, 2003b, Volume 42, 605-615.
- Halvorsen, I.J., Skogestad, S., 'Minimum energy consumption in multicomponent distillation. 2. More than three products and generalised Petlyuk arrangements', *Ind. Eng. Chem. Res.*, 2003c, Volume 42, 616-629.
- Henley, E.J., Seader, J.D., 'Equilibrium-Stage Separation Operations in Chemical Engineering', John Wiley & Sons, 1981.
- Hewitt, G., Quarini, J., Morell, M., 'More efficient distillation', *The Chemical Engineer*, 21 Oct. 1999
- King, C.J., 'Separation Processes', 2nd edition, McGraw-Hill Book Co., 1980.
- Rev, E., Emtir, M., Szitkai, Z., Mizsey, P., Fonyó, Z., 'Energy savings of integrated and coupled distillation systems', *Computers and Chemical Engineering*, 2001, 25, 119-140.
- Skogestad, S., 'Dynamics and control of distillation columns: A tutorial introduction', *Trans IChemE*, 1997, Vol. 75, Part A, 539-562.
- Skogestad, S., 'Prosessteknikk', 2nd edition, Tapir Akademisk Forlag, Trondheim, Norway, 2003.